COMPARISON OF THE ASAR ALTERNATIVE POLARISATION MODE TO FULL POLARIMETRIC ACQUISITION FOR LAND USE ESTIMATION OVER TROPICAL REGIONS

Cédric Lardeux, Pierre-Louis Frison, Céline Tison, D Deleflie, Jean-Claude Souyris, Jean-Paul Rudant, Benoit Stoll

COMPARISON OF THE ASAR ALTERNATIVE POLARISATION MODE TO FULL POLARIMETRIC ACQUISITION FOR LAND USE ESTIMATION OVER TROPICAL REGIONS

C. Lardeux[(1)], P.-L. Frison [(1)], C. Tison[(2)], D. Deleflie, J.-C. Souyris[(2)], J.-P. Rudant[(1)], B. Stoll[(3)]

[(1)]Université de Marne la Vallée, laboratoire G2I-IFSA, 5 boulevard Descrates, 77 454 Marne la Vallée Cedex 2
Email: cedric.lardeux@univ-mlv.fr
[(2)]Centre National d'Etudes Spatiales, DCT/SI/AR, 18 avenue Edouard Belin, 31 401 Toulouse Cedex 4, France
Email: celine.tison@cnes.fr
[(3)]Université de Polynésie Française, B.P. 6570 98702 FAA'A Tahiti - Polynésie Française
Email : benoit.stoll@upf.pf

ABSTRACT

This study comes within the framework of the global cartography and inventory of the Polynesian landscape. An AIRSAR airborne acquired fully polarimetric data in L band, in August 2000, over the main Polynesian Islands. This study focuses on Tubuai Island, where several ground surveys allow the validation of the different results. While they preserve some of the polarimetric information as those that would be recorded by a full polarimetric (FP) radar sensor, compact polarimetry (CP) architectures are relevant for systems constraints reduction. For example the ASAR Alternate Polarization mode provides the intensities recorded in 2 linear polarization channels with no phase information between them. On the other hand an other CP mode, called the *"π/4"* mode, has been proposed due to its optimum compromise between system architecture and polarimetric information preservation especially when natural surfaces are concerned. These 2 CP configurations are simulated from AIRSAR data in order to investigate their potential with respect to FP for land use classification. The classification method retained is the SVM (Support Vector Machine) algorithm due to its ability to handle linearly non separable cases by using the kernel method. In particular, it is well suited for combining numerous heterogeneous indicators such as intensity channels, polarimetric descriptors, or textural parameters.
The results show that for full polarimetric data, the SVM classification performance when only the elements of the polarimetric coherence matrix are involved is comparable to the Wishart classification one. The addition of polarimetric indices improves significantly the classification. On the other hand when *"π/4"* mode is simulated, the overall classification performance is decrease of 8% than those observed with full polarimetric data in reason of a higher confusion for some forest classes (Pinus, Falcata and Guava). However, the discrimination between forest, low vegetation and no vegetation area is quite similar to the FP mode. Moreover, the *"π/4"* mode shows much better performance for the present land use discrimination than the ASAR alternate polarization mode that are not really able to discriminate the forest species.

1. INTRODUCTION

Radar data are of particular interest over tropical areas such as the French Polynesian Islands because of persistent cloudy weather. Fully polarimetric SAR data were acquired in L and P bands over the main Polynesian islands. The overall goal of this study is to assess the potential of such fully polarimetric SAR data for land-use cartography and to compare in the same way different partial polarimetric mode like *"π/4"* mode [1] or the Envisat alternate polarization mode. When dealing with classification methods applied to full polarimetric data, the Wishart classification [1] [2] or algorithm based on polarimetric decomposition such as the H/A/α decomposition [3] are generally used. In order to integrate heterogeneous polarimetric descriptors (*i.e.* not only the coherence matrix used in the Wishart classification, but also other polarimetric descriptors, such the H/A/α parameters), it is proposed to use the SVM (Support Vector Machine) classification method [4]. It is especially well suited to handle linearly non separable case by using Kernel functions. It has been mostly applied to hyperspectral remote sensed data and few studies have also been conducted with SAR data [5][6]. The study area and radar data are presented in the second part of this paper. The third part details the SVM algorithm and describes the polarimetric indices used to define the different SV that are suitable to each polarimetric modes involved. The results are presented in the last part of the paper.

2. STUDY AREA AND DATASET

2.1. Study area

French Polynesia islands are located at the middle of the South Pacific Ocean. They are quickly evolving in the tourism industry, and from the economic and geostrategic points of view. They are thus subject to a strong environmental planning leading to landscape changes as well as to the introduction of invasive

species. This study comes within the framework of the global cartography and inventory of the Polynesian landscape. We focus on data acquired over the Tubuai Island, in the Australes Archipelago at the South of French Polynesia. Tubuai is a 45 km^2 island with a population of about 6000 inhabitants. It is particularly relevant because of its great landscape diversity: several types of forests, agricultural fields, and residential areas. The objective is to estimate different land use class, in particular by discriminating different forest types containing four classes: *Hibiscus tiliaceus* (also called Purau), *Pinus Caribeae* (also called Pinus), *Paraserianthes Falcataria* (also called Falcata). The 2 other classes are the one labelled "Low Vegetation", including fern lands, swamps vegetation, and few crops and the "Other" class including bare fields, low grass fields. Several ground surveys has been carried out, and a Quickbird image acquired in August 2004 is also available to supply an accurate validation data set over the entire island.
The class are summarized in Table 1 with the number of pixels of the radar image associated to training and control classes.

Table 1: Training and testing samples number used for the Tubuai Island classification

Class	Training samples	Control samples
Pinus	5330	5330
Falcata	2696	2696
Purau	6202	6202
Guava	365	365
Low Vegetation	7897	7897
Other	4457	4457

2.2. Airsar data

An AIRSAR airborne mission took place in August 2000 over the main Polynesian islands. The AIRSAR data were acquired over Tubuai along 2 passes in reverse path, in Polsar mode. The data set used in this study consists in full polarimetric data in L (λ = 23 cm) and P (λ = 67cm) bands with an additional C band channel (λ=5.7cm) in VV polarization. Full polarimetric data are delivered in MLC (Multi Look Complex) format, corresponding to about 9 looks, with a resolution of 5 meters. The relative phase of the original data has been calibrated following [7] and an intensity bias has been corrected both in L and P bands values.

3. Methodology

3.1. Support Vector Machine

A brief description of SVM is made below and more details can be found in **REF** [4].

- **Linear case** :

Let us consider a two class classification problem with N training samples. Each sample is described by a Support Vector (SV) X_i composed by the different "bands" with n dimension. The label of a sample is Y_i. For a two classes case we consider the label -1 for the first class and +1 for the other.
The SVM model ω describes the optimal hyperplane which separate the two classes (Figure 1). The classification function f is consequently defines as $f(x) = \mathrm{sign}(\langle \omega, X \rangle + b)$

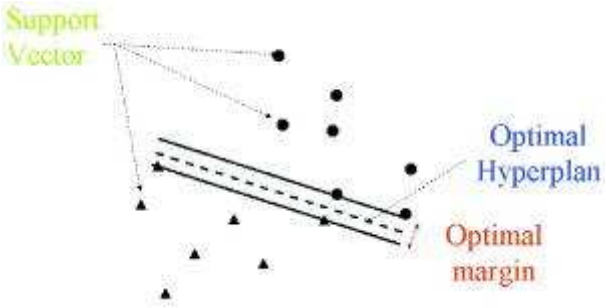

Figure 1. SVM Classifier-Linear case

The sign of f(x) gives the label of the sample. The goal of the SVM is to maximize the margin between the optimal hyperplane and the support vector. So we search for the $\min(\frac{\|\omega\|}{2})$ .To do this, it is more easier to use the Lagrange multiplier. The problem comes to solve:

$$f(x) = Sign(\sum_{i=1}^{Ns} y_i.\alpha_i.\langle x, x_i \rangle + b) \quad (1)$$

Where α_i is the Lagrange multiplier.

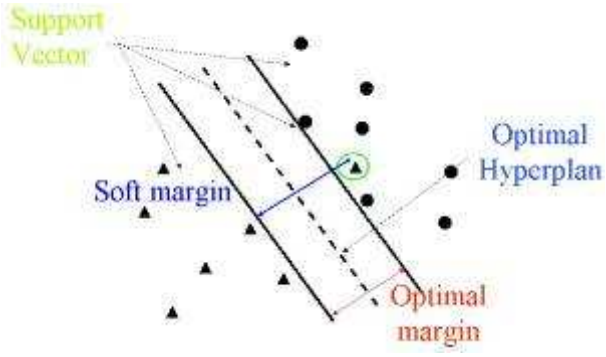

Figure 2. SVM Classifier-Nonlinear case

Soft margin enables to get robust to noisy training data set.

- **Nonlinear case :**

When classification problem is not linear (Figure 2) the training vectors are projected into a "feature space" H of

higher dimension through the feature function Φ ($\Phi : \Re^n \mapsto H$). In H, the data become linearly separable. Actually, in SVM model, the function Φ is replaced by its scalar product, the Kernel function: $K(x, x_i) = \langle \Phi(x), \Phi(x_i) \rangle$. Then the new classification function is equal to:

$$f(x) = Sign(\sum_{i=1}^{Ns} y_i.\alpha_i.K(x, x_i) + b) \quad (2)$$

Three kernels are commonly used:

- The polynomial kernel
  $K(x, x_i) = (\langle x, x_i \rangle + 1)^p$
- The sigmoid kernel
  $K(x, x_i) = \tanh(\langle x, x_i \rangle + 1)$
- The RBF kernel

$$K(x, x_i) = \exp - \frac{|x - x_i|^2}{2\sigma^2}$$

The RBF kernel has been selected in this work through empirical considerations. A future work would be to develop a new kernel accounting for the distribution of the data, such the one is due to the presence of speckle in SAR data.

- Multiclass case :

The principle of SVM has been developed for a two class problem but it has been easily extended to a multi-class problem with several algorithms. Among them, there are:
the "One Against All" (OAA) and the "One Against One" (OAO) algorithms.

If we consider a problem with K class:
The OAA algorithm consists in the construction of k hyperplane that separate respectively one class and the (k-1) other classes.
The OAO algorithm consists in the construction of $\frac{k(k-1)}{2}$ hyperplane which separate each pair of classes.
In the two cases the final label is that mainly chosen. After several tests, the OAO algorithm has been retained as well as the RBF kernel with σ=0.5 and the cost parameter equal to 1000 (soft margin).
The Libsvm library has been used [8].

3.2. Polarimetric indices

Several Support Vectors have been defined for full polarimetric data to measure the impact of the different polarimetric indicators. On the one hand, for comparison with Wishart classification, a support vector (referenced *SV1* hereafter) is made up by the 9 elements only of the coherency matrix T. This latter is constructed from the scattering vector k_p expressed in the Pauli basis as follows:

$$k_p = \frac{1}{\sqrt{2}} \begin{pmatrix} S_{HH} + S_{VV} \\ S_{HH} - S_{VV} \\ 2.S_{HV} \end{pmatrix}, [T] = k_p.k_p^{*T} \quad (3)$$

S_{wx} denotes the scattering matrix element corresponding to the *w*/*x* polarization for the receiving/transmitting wave (*w*, *x* referring to horizontal, H, or vertical, V, linear polarization)
On the other hand, a second support vector, *SV2*, is built with the addition of different polarimetric indices. These are detailed hereafter and summarized in Table 2:

- The intensities in the 2 co- and 1 cross- polarized channel in linear and circular polarization:

$$I_{wx} = |S_{wx}|^2 \quad (4)$$

where *w* and *x* refer to H, V, left, L, and/or right, R, circular polarization.

- The Span:

$$SPAN = I_{HH} + 2\,I_{HV} + I_{VV} \quad (5)$$

- The texture is taken into account through the coefficient of variation $c_v = \frac{\sigma}{\mu}$, σ and μ are representing the standard deviation and mean of the intensities in the linear and circular polarization (3) computed over a 5x5 neighbourhood.
- The ratio between the following intensities:

$$\frac{I_{HV}}{I_{HH}}, \frac{I_{HV}}{I_{VV}}, \frac{I_{HH}}{I_{VV}}, \frac{I_{LL}}{I_{LR}} \quad (6)$$

Table 2: Support Vector configuration

SV1	# el^{ts}	SV2	# el^{ts}
T elements	9	T elements	9
		I_{HH}, I_{HV}, I_{VV}, I_{LL}, I_{LR}, I_{RR}	6
		$SPAN = \|S_{HH}\|^2 + 2\|S_{HV}\|^2 + \|S_{VV}\|^2$	1
		$c_{v\text{-}HH}$, $c_{v\text{-}HV}$, $c_{v\text{-}VV}$, $c_{v\text{-}LL}$, $c_{v\text{-}RR}$, $c_{v\text{-}LR}$,	6
		$\frac{I_{HV}}{I_{HH}}, \frac{I_{HV}}{I_{VV}}, \frac{I_{HH}}{I_{VV}}, \frac{I_{LL}}{I_{LR}}$	4
		$\|\rho_{HH-VV}\|, \|\rho_{HV-VV}\|, \|\rho_{HV-HH}\|$ $\|\rho_{LL-LR}\|, \|\rho_{RR-LR}\|, \|\rho_{LL-RR}\|$	6
		P_{min}	1
		Deg_{min}	1
		m and γEuler parameters :	2
		H/A/α	3
Total	9		39

- The modulus of the degree of coherence, $|\rho_{HH-VV}|, |\rho_{HV-VV}|, |\rho_{HV-HH}|, |\rho_{LL-LR}|, |\rho_{RR-LR}|, |\rho_{LL-RR}|$ computed as follow:

$$|\rho_{wxyz}| = \left| \frac{\langle S_{wx}.S_{yz}^{*} \rangle}{\sqrt{\langle |S_{wx}|^2 \rangle . \langle |S_{yz}|^2 \rangle}} \right| \qquad (7)$$

where w, x, y, z, stands for H, V, L and R polarization

- The minimum power of the backscattered wave, P_{min}, for all the polarization configuration of the emitted wave.
- The minimum of the degree of polarization of the received wave $\partial P_{\min}$ for all the polarization configurations of the emitted wave. The degree of polarization is defined as

$$\partial P = \frac{\sqrt{S_2^2 + S_3^2 + S_4^2}}{S_1} \qquad (8)$$

S_1, S_2, S_3, S_4 being the 4 elements of the Stokes vector.

- The 2 Euler parameters m and γ representing respectively the magnitude and the polarisability of the resolution cell. Details about their calculation from the Stokes parameters are given in [9].
- The 3 parameters $H/A/\alpha$ representing the entropy, the scattering mechanism, and the anisotropy [3])

At the exception of the coefficient of variation C_V, all the other polarimetric indices have been estimated after the application of a polarimetric filter [10] to original data.

3.3. Compact Polarimetry: the "$\pi/4$" Mode

The "$\pi/4$" mode consists in a transmitter polarization either circular or oriented at 45°, and in receivers that are in horizontal and vertical polarizations with respect to the line of sight.

Due to some symmetry properties (reflection, rotation, azimuthal) for natural media, some hypothesis could be made to reconstruct the full polarimetric information. More details are given in [1]. In particular, it is shown that this mode is similar to FP modes when (8) is verified.

$$\langle S_{HH}.S_{HV}^{*} \rangle = \langle S_{HV}.S_{VV}^{*} \rangle = 0 \qquad (8)$$

This property is generally observed over distributed target, such as vegetated areas.

Consequently, some polarimetric parameters lose their signification or become redundant with other. For example, the circular intensities I_{LL} and I_{RR} are equal. In the same way, the degree of coherence ρ_{llrr} has no more interest, as well as the degree of coherence involving the cross linear polarisation HV that is equal to zero. The primitives defining the Support Vector SV3, adapted from SV2 to the "$\pi/4$" mode is summarized in Table 3.

Table 3: Support Vector configuration of the "$\pi/4$" mode

SV3	# el^{ts}
T elements	7
I_{HH}, I_{HV}, I_{VV}, I_{LL}, I_{LR}	5
$SPAN = \|S_{HH}\|^2 + 2\|S_{HV}\|^2 + \|S_{VV}\|^2$	1
$c_{v\text{-}HH}$, $c_{v\text{-}HV}$, $c_{v\text{-}VV}$, $c_{v\text{-}LL}$, $c_{v\text{-}LR}$,	5
$\frac{I_{HV}}{I_{HH}}, \frac{I_{HV}}{I_{VV}}, \frac{I_{HH}}{I_{VV}}, \frac{I_{LL}}{I_{LR}}$	4
$\|\rho_{HH-VV}\|, \|\rho_{LL-LR}\|$	2
P_{min}	1
Deg_{min}	1
m and γ Euler parameters :	2
$H/A/\alpha$	3
Total number of primitives	31

3.4. *Alternate polarization* Mode

The Alternate Polarization mode (AP) provided by ASAR sensor consists in the emission of one linear polarisation with the reception in two linear polarizations. Consequently, the result is a couple of intensities HH and HV, VV and HV or HH and VV. The associated primitives defining the SV SV4 are summarized in Table 4.

Table 4: Support Vector configuration of the AP mode (*w*, *x* referring to horizontal, H, or vertical, V, linear polarization).

SV4	# el^{ts}
I_{wx}, I_{wx}	2
$SPAN = \|S_{wx}\|^2 + \|S_{wx}\|^2$	1
$c_{v\text{-}wx}$, $c_{v\text{-}wx}$	2
$\frac{I_{wx}}{I_{wx}}$	1
Total number of primitives	6

4. Results and discussion

4.1.1. Full Polarimetric data

In order to assess the suitability of the SVM algorithm to polarimetric SAR data, the SVM with the SV1 support vector has been compared to the Wishart classification [2] over an extract.

The overall performance of the classification is given by the Kappa coefficient, κ; while the Producer Accuracy is used to estimate the performance for the different classes [12].

The SVM algorithm shows similar results as Wishart for the L band (κ=72% and κ=67% respectively) and the P band (κ=63% and κ=66% respectively). It can be

noticed that a high confusion is observed between the different forest types for both bands that is particularly marked for the Wishart algorithm.
In a second step, the SV2 Support Vector has been used in order to assess the contribution of the polarimetric indices. Results are presented in Table 5.

Table 5: SVM classification results with SV2: the Producer Accuracy (%) is given for the different classes, and the overall performance is given by κ

	L	P	L+P	L+P+C_{VV}
Pinus	87	87	96	99
Falcata	84	74	86	89
Purau	88	89	94	97
Guava	90	76	83	83
Low Vegetation	99	99	99	99
Other	98	97	98	98
κ *(%)*	91	87	93	94

The addition of polarimetric indices improves significantly the SVM classification results, with $\kappa = 91$ % and $\kappa = 87$ % for L and P band. These values have to be compared with those obtained with SV1 Support Vector ($\kappa = 72$ % and $\kappa = 63$ % for L and P band respectively). Both bands present as a whole the same performance with still significant confusion between the different forest types especially for the P band.
When the L and P bands are combined, leading to a Support vector of 78 components, there is an average increase of 4% for the κ value that reaches 93%. The forest classes are much better discriminated particularly for the *Pinus* (PA = 96 %) and the *Purau* (PA = 94 %). But the *Falcata* and the *Guava* shows still high confusion. Finally, the addition of the C band-VV polarisation intensity data (leading to a 79 components Support Vector) improve lightly the overall results, with κ = 94%. However, it increases significantly the *Purau* and the *Pinus* discrimination, while there is still persistent confusion concerning the *Guava*.

4.1.2. $\pi/4$ configuration

Results obtained in different wavelength configuration for the *"$\pi/4$"* mode with the SV3 Support Vector (cf. Table 3) are given in Table 6. The result show a fall of 8% and 7% of the global accuracy for L and P band respectively. It's mainly due to the forest species except the *Purau*, contrary to the *Low vegetation* and *Other classes*. However, when the different bands are combined, and more especially with the addition of the C band-VV polarisation intensity, the results are similar to the FP mode.

Table 6: SVM classification results with SV3: the Producer Accuracy (%) is given for the different classes, and the overall performance is given by κ (%).The indices give the difference between FP and "$\pi/4$" mode.

	L	P	L+P	L+P+C_{VV}
Pinus	73 $_{-14}$	78 $_{-9}$	90 $_{-6}$	99 $_{0}$
Falcata	70 $_{-14}$	61 $_{-13}$	79 $_{-7}$	87 $_{-2}$
Purau	85 $_{-4}$	86 $_{-2}$	91 $_{-3}$	96 $_{-1}$
Guava	80 $_{-10}$	67 $_{-9}$	79 $_{-4}$	80 $_{-3}$
Low Vegetation	98 $_{-2}$	97 $_{-2}$	99 $_{0}$	99 $_{0}$
Other	96 $_{-2}$	94 $_{-3}$	97 $_{-1}$	97 $_{0}$
κ *(%)*	83 $_{-8}$	80 $_{-7}$	89 $_{-4}$	93 $_{-1}$

4.1.3. Alternate polarizations modes

Results obtained for the different ASAR Alternate Polarization modes, with the SV4 Support Vector configuration (see Table 4) are presented in Table 7 for L and P band and in Table 8 for the different combination of the wavelength. Results are given for the 3 different couples of polarization and their combination (this later corresponding for example to different acquisition dates).

Table 7: SVM classification results with DP and AP modes for L band: the Producer Accuracy (%) is given for the different classes, and the overall performance is given by κ (%).

	HH/HV		VV/HV		HH/VV		HH/HV/VV	
Band	L	P	L	P	L	P	L	P
Pinus	56	77	58	75	56	75	56	75
Falcata	28	3	3	5	29	4	32	10
Purau	79	85	79	85	78	86	80	86
Guava	21	7	15	16	20	12	26	22
Low Vegetation	95	92	96	94	92	93	97	94
Other	89	83	85	81	90	83	89	84
κ *(%)*	60	57	55	58	60	57	62	61

For L as well as P bands, when only 2 polarizations channels are concerned, results show that only three different landscape can be discriminated: forest, *Low vegetation* and *Other classes*. Indeed the different forest classes reveal some confusion. This is particularly obvious for *Falcata* and *Guava* species, with Producer Accuracy values lower than 32% in all configuration.
When the 3 linearly polarized channels are combined (Table 7, last 2 columns), accuracies are increased, but confusion for the *Falcata* and the *Guava* is still observed.

For each configuration, when the L and P band are combined (see Table 8), the results show less confusion between the forest classes, particularly for *Pinus* and *Purau*. The addition of the Cvv band increases this phenomena.

Table 8: SVM classification results with ASAR AP modes: the Producer Accuracy (%) is given for the different classes, and the overall performance is given by κ(%).

	HH HV		VV HV		HH VV		HH HV VV	
Band	L+P	L+P Cvv	L+P	L+P Cvv	L+P	L+P Cvv	L+P	L+P Cvv
Pinus	78	98	79	97	78	98	78	98
Falcata	42	76	23	64	43	73	49	76
Purau	84	93	85	93	84	94	85	93
Guava	54	63	46	54	49	61	57	67
Low Vegetation	97	98	96	98	95	97	98	98
Other	91	93	90	92	92	92	94	95
κ (%)	74	86	69	82	73	85	76	87

5. Conclusion

This study shows that the SVM classification algorithm is well suited for full polarimetric data with similar accuracy as Wishart classification. The possibility to add different polarimetric or textural indices makes the SVM algorithm make it especially interesting as the overall performance giving by the κ value increases of about 20% with respect to classification involving only the elements of the matrix of coherence. Moreover, the simulation of compact architecture like the "*π/4*" mode shows comparable results to full polarimetric SVM classification except for specific forest species. On the other hand, when only one band is concerned, results obtained with ENVISAT Alternate Polarization simulations (HH/VV, HH/HV, HH/HV/VV) shows a quite good discrimination between *Forest*, *Low vegetation* and *Other classes* area while significant confusion is observed between the different forest species. Results obtained for the "*π/4*" mode show significant improvements. In particular it allows a better discrimination between the different forest species.

Acknowledgment

The authors are very grateful to Jean-Yves Meyer for the survey mission and we would like to thank the Government of French Polynesia and its Urbanism Department for providing the AirSAR, MASTER and Quickbird data required for this study.

Fonds cartographiques du service de l'urbanisme

References

[1] J.-C. Souyris, P. Imbo, R. Fjørtoft, S. Mingot, J.-S. Lee, *Compact Polarimetry Based on Symmetry Properties of Geophysical Media: The π/4 Mode*, IEEE Trans. Geosci. Remote Sens., vol. 43, no. 3, Mar. 2005. Page(s):634 – 646

[2] J. S. Lee, M. R. Grunes, R. Kwok, *Classification of multi-look polarimetric SAR imagery based on complex Wishart distribution*, Int. J. Rem. Sens., vol. 15, n° 11, 1994, 2299-2311.

[3] S. R. Cloude, E. Pottier *A Review of Target Decomposition Theorems in Radar Polarimetry*, IEEE TGRS, vol. 34, no. 2, pp 498-518, Sept. 1995.

[4] C. J. Burges, *A tutorial on support vector machines for pattern recognition*, in Data mining and knowledge discovery, U. Fayyad, Ed. Kluwer Academic, 1998, pp. 1-43.

[5] S. Fukuda and H. Hirosawa *Support Vector Machine Classification of Land Cover: Application to Polarimetric SAR Data* in Geoscience and Remote Sensing Symposium, 2001. IGARSS '01. IEEE 2001 International, 9-13 July 2001 Page(s):187 - 189 vol.1

[6] G. Mercier and F. Girard-Ardhuin, *Unsupervised Oil Slick Detection by SAR Imagery using Kernel Expansion*, Geoscience and Remote Sensing Symposium, 2005. IGARSS '05. Proceedings. 2005 IEEE International vol.1, 25-29 July 2005 Page(s):494 – 497

[7] H. A. Zebker, J. J. van Zyl, and D.H.Held, *Imaging radar polarimetry frow waves synthesis*, J.Geophy. Res, vol. 91, no B5. pp. 683-701, Jan. 1987.

[8] Libsvm is available at http://www.csie.ntu.edu.tw/cjlin/libsvm

[9] D. Laurent, E. Pottier, and J. Saillard *The Euler vector : a polarimetric descriptor of the ocean surface*, journal of Electromagnetic Waves and Applications. vol. 9, n1/2 pp 217-240, 1995

[10] J. S. Lee, M. R Grunes, G. de Grandi,, *Polarimetric SAR speckle filtering and its implication for classification*, IEEE Trans. Geosci. and Rem. Sens., vol. 37, n0 5, 1999, 2362-2373

[11] ESA,*PolSarPro*, available at http://earth.esa.int/polsarpro/

[12] T. M. Lillesand and R. W. Kiefer, *Remote sensing and Image interpretation*, 3rd ed., New York: Wiley, 1993.